Hot Paper

Monomeric gold hydrides for carbon dioxide reduction: ligand effect on the reactivity

Elisa Rossi,[a] Diego Sorbelli,*[b, c] Paola Belanzoni,[b, d] Leonardo Belpassi,[d] and Gianluca Ciancaleoni*[a, e]

We analyzed the ligand electronic effect in the reaction between a $[LAu(I)H]^{0/-}$ hydride species and CO_2, leading to a coordinated formate $[LAu(HCOO)]^{0/-}$. We explored 20 different ligands, such as carbenes, phosphines and others, carefully selected to cover a wide range of electron-donor and -acceptor properties. We included in the study the only ligand, an NHC-coordinated diphosphene, that, thus far, experimentally demonstrated facile and reversible reaction between the monomeric gold(I) hydride and carbon dioxide. We elucidated the previously unknown reaction mechanism, which resulted to be

concerted and common to all the ligands: the gold–hydrogen bond attacks the carbon atom of CO_2 with one oxygen atom coordinating to the gold center. A correlation between the ligand σ donor ability, which affects the electron density at the reactive site, and the kinetic activation barriers of the reaction has been found. This systematic study offers useful guidelines for the rational design of new ligands for this reaction, while suggesting a few promising and experimentally accessible potential candidates for the stoichiometric or catalytic CO_2 activation.

Introduction

The concentration of carbon dioxide (CO_2), a well–known greenhouse gas, is increasing in the atmosphere,[1] prompting the need for its effective and sustainable utilization. In fact, this molecule possesses significant potential as an abundant and economically viable C1 building block. However, its utilization as a feedstock is non–trivial due to its high oxidation state, thermodynamic stability, and kinetic inertness. To overcome these obstacles, researchers exploited the known reactivity of bases to activate and chemically transform carbon dioxide. Indeed, various catalytic processes, such as the hydrogenation to formic acid or methanol, involve the reaction with basic metal hydride species through insertion of CO_2 into the metal–hydrogen bond of a catalyst.[2,3] This strategy offers promising

avenues to overcome the difficulties associated with CO_2 activation and conversion, enabling its transformation into valuable chemicals.

Based on these considerations, the CO_2 activation *via* insertion into metal–hydrogen bond has been extensively investigated, particularly by employing computational approaches to elucidate the fundamental aspects of its mechanism.[2,3–6] In general, the molecular events are a nucleophilic attack of the hydride moiety on the C atom of CO_2, while one oxygen binds to the metal giving the O-bound formate product. Depending on the synchronicity of these two events, a concerted or a two-step mechanism has been proposed.[7–9] The former is favored for complexes with unsaturated metal coordination, whereas the latter is preferred when the metal center is sterically hindered by its ligands.

Late-transition-metal complexes offer the advantage of relatively weak metal-oxygen bonds, thus facilitating two-step mechanisms.[2] Notably, hydrides based on noble metals, such as rhodium, iridium, palladium, platinum, and ruthenium, have been fruitfully utilized in catalyzing this kind of carbon dioxide conversions.[2,10–12] When gold is involved, the challenging nature of hydrides preparation has been a limiting factor for further applications for a long time.[13] An N-heterocyclic carbene (NHC) ligand proved to be able to stabilize the hydride group, and the resulting [(IPr)AuH] (IPr = 1,3-bis(2,6-diisopropyl-phenyl) imidazol-2-ylidene) complex exhibited reactivity towards dimethyl acetylenedicarboxylate, ethyl diazoacetate, and O_2,[14–16] but not with CO_2. On the contrary, the NHC-stabilized diphosphene gold(I) hydride (1,[17] Scheme 1) demonstrated facile and reversible reaction with carbon dioxide[17,18] by exposing a toluene solution of the complex to gaseous CO_2, and the release was demonstrated to occur spontaneously. However, to the best of our knowledge, the detailed mechanistic aspects of this reaction remain unexplored.

[a] E. Rossi, Prof. Dr. G. Ciancaleoni
     Department of Chemistry and Industrial Chemistry, University of Pisa, Pisa, I-56124, Italy

[b] Dr. D. Sorbelli, Prof. Dr. P. Belanzoni
     Department of Chemistry, Biology and Biotechnology, University of Perugia, Perugia, I-06123, Italy

[c] Dr. D. Sorbelli
     Pritzker School of Molecular Engineering, University of Chicago, 5640 South Ellis Avenue, Chicago, IL, 60637, US
     E-mail: dsorbelli@uchicago.edu

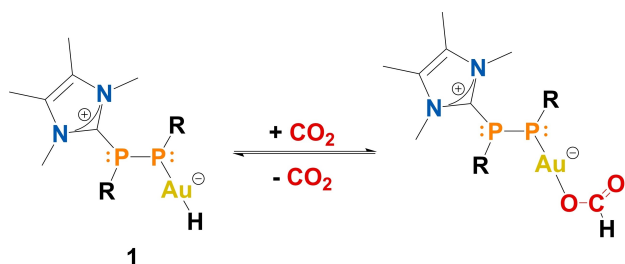[d] Prof. Dr. P. Belanzoni, Dr. L. Belpassi
     CNR Institute of Chemical Science and Technologies "Giulio Natta" (CNR-SCITEC), c/o Department of Chemistry, Biology and Biotechnology, University of Perugia, Perugia, I-06123, Italy

[e] Prof. Dr. G. Ciancaleoni
     CIRCC, Bari, Italy

Chemistry–A European Journal

Research Article
doi.org/10.1002/chem.202303512

Chemistry Europe
European Chemical
Societies Publishing

Scheme 1. Reversible reaction of Au(I)-hydride **1** ($R = 2,6\text{-Mes}_2\text{–C}_6H_3$) with CO_2.

The intriguing and relatively unexplored reactivity between gold hydrides and carbon dioxide has motivated our investigation on the influence of the ligand on this reaction. Hydride complexes of the type [LAuH], with L = ligand, have been considered in our study which encompasses a set of 20 different ligands (sketched in Scheme 2), carefully selected to cover a wide range of electron–donor and -acceptor properties. Within the general NHC structure, we considered modifications on the groups bonded to the nitrogen atoms (**NHC**, **H_H_NHC**), on the substituents on the NHC backbone (**4H_NHC**, **O_NHC**⁻,[19] **Me₃B_NHC**⁻,[20] **H₃B_NHC**⁻, **F₃B_NHC**⁻, **ox_NHC**[21]), and an acyclic carbene (**CN₂Me₄**). For the phosphine ligands, we selected a **PR₃** structure, incorporating fluorine atoms (**PF₃**), methyl or phenyl groups (**PMe₃**, **PPh₃**), and **PMe₂**⁻. Additionally, we included the [**NONAl**]⁻ ligand in our investigation, as it has previously demonstrated unconventional properties in combination with gold, particularly concerning carbon dioxide insertion reactions.[22–25] **NMe₂**⁻, **Cl**⁻, **CO**, **CN**⁻ were used as model ligands to stress the influence on the target reaction with enhanced negative charge density or π acceptor ability. Finally, we included the experimental complex **1** (Scheme 1)[17] introducing some structural simplifications (obtaining **1′**, reported in Scheme 2) with the aim of reducing the computational cost, while not altering the reactivity. We replaced the
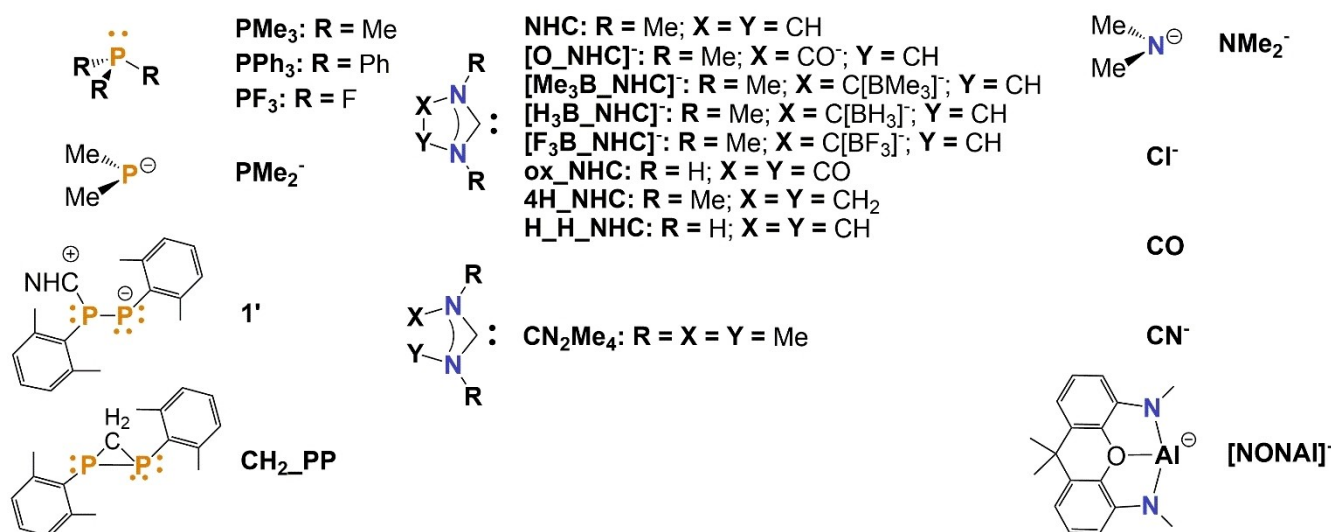
two $2,6\text{-Mes}_2\text{–C}_6H_3$ moieties with two 2,6-dimethylbenzenes, maintaining the influence of the aromatic group, while the NHC ligand was simplified by just substituting the two methyl groups on the backbone with hydrogen atoms. We also introduced a simple variation of this diphosphene ligand by substituting the NHC with a different carbene, namely the CH_2, obtaining the **CH₂_PP** diphosphene.

Obviously, some ligands listed in Scheme 2 serve only as models aimed at a deeper understanding of the process, such as **CH₂_PP**, **PF₃**, or **PMe₂**⁻. In contrast, also experimentally accessible ligands (or analogues) have been considered, like [**O_NHC**]⁻ and [**Me₃B_NHC**]⁻, even if, to the best of our knowledge, they have been not yet tested in the reaction under study.

We decided to employ the Charge Displacement analysis[26,27] via Natural Orbitals for Chemical Valence (CD–NOCV) approach,[28–33] which enabled us to both characterize the ligand–metal and metal–hydride bonds and quantitatively and visually assess the nature of the complex-CO_2 interaction. This method already proved to effectively decompose not only the metal–ligand bond components, but also to find correlations between the latter and second–sphere interactions.[34–36] Based on this tool, we could identify a correlation between the Gibbs activation barrier for the CO_2 insertion reaction into the Au–H bond and the electronic structure of the complexes. With these results in hand, we aim to propose theoretical guidelines for the rational design and development of monomeric Au(I) hydrides possessing the capability to reduce CO_2 to formate anion. Furthermore, in certain cases, it is possible to predict the reversibility of this reaction, paving the way to novel catalysts.

Computational Details

All complexes were optimized in vacuo using the ORCA software,[37] version 5.0.1.[38] In order to account for relativistic effects, we used the ZORA approach,[39–41] employing the ZORA–def2–TZVP basis set for all the atoms, along with the SARC–ZORA–TZVP basis set for

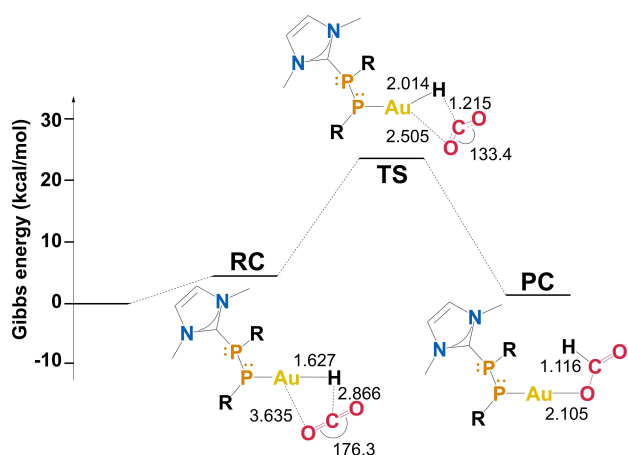**Scheme 2.** List of all the ligands L in the [LAuH] complexes investigated in this study.

RIGHTS LINK

Chemistry–A European Journal

Research Article
doi.org/10.1002/chem.202303512

**Chemistry
Europe**
European Chemical
Societies Publishing

Figure 1. Free energy reaction profile and chemical structures for the CO_2 insertion into the Au–H bond in the **1'** complex (R = 2,6-dimethylbenzene; **RC** = reactant complex, **TS** = transition state, and **PC** = product complex). The energy reference is the sum of the energies of **1'** gold hydride and CO_2. Selected interatomic distances (Å) and bond angles (degrees) are given with the molecular structures.

gold.[42] We utilized the BP86 functional,[43,44] the RIJCOSX approximation, and we included dispersion effects *via* the D3BJ scheme.[45,46] All stationary points were characterized to ensure the absence of imaginary frequencies for reactants and products, or the presence of a single imaginary frequency for transition states. The effect of solvation (toluene) was evaluated for representative complexes with the COSMO model[47] and it was found to produce a limited effect on the mechanism and activation barriers (see Table S5).

The same computational protocol was utilized for the Energy Decomposition Analysis (EDA)[48] and Charge Displacement via Natural Orbitals for Chemical Valence (CD–NOCV) analyses, which were conducted using the ADF code,[49] version 2016.104. The numerical integration to obtain the CD–NOCV curves has been carried out using PYCUBESCD suite.[50,51]

Computational details about EDA and CD–NOCV methodologies can be found in the Supporting Information.

Results and Discussion

As illustrated in Scheme 1, complex **1** nicely inserts CO_2 into the Au–H bond. Understanding the reaction mechanism is the first step to our ultimate goal, which is to find guidelines for an effective ligand design.

We found that, in agreement with the low hindrance around the metal, the process occurs *via* a concerted transition state, in which the hydrogen atom binds to the carbon atom of CO_2 while simultaneously breaking the Au–H bond (Figure 1). At the same time, one oxygen of CO_2 starts to form a bond with the gold center, leading to the subsequent relaxation and formation of the formate product. Initially, carbon dioxide weakly interacts with the hydride, forming the reactant complex **RC**. The concerted transition state (**TS**) requires an activation barrier of 24.0 kcal/mol, coherently with the experimental feasibility of the process.[17] At the **TS**, CO_2 exhibits a significant bending (133.4° for the OĈO angle) being at a relatively close distance

from Au (2.505 Å) and very close to the H atom (1.215 Å). As a result, the Au–H bond is elongated, compared to its length in the **RC**, and the P–Âu–H angle deviates from the initial configuration (160.1° at the **TS**, 172.9° at the **RC**, and 173.7° in the isolated hydride **1'**). The formation of Au–O and H–C bonds, along with the complete breaking of the Au–H interaction results in the formation of the formate product **PC**. Remarkably, the free energy of the product is nearly identical to that of the initial reactants (+1.2 kcal/mol), in agreement with the experimental reversibility of this reaction. The free energy profile for the CO_2 insertion into the Au–H in the experimentally accessible complex **1'** is shown in Figure 1.

This reactivity can be nicely rationalized in terms of molecular orbitals (MOs) of CO_2 and **1'**. The main results of the NOCV analysis at TS, reported in Figure 2, clearly display that the main driving force ($\Delta\rho_1$) of the $[CO_2]$-$[1']$ interaction is represented by the charge transfer from the Au–H bonding MO, also including contribution from the P–Au σ bond, towards the empty π* LUMO of CO_2. This picture is strongly reminiscent of the interaction scheme depicted for CO_2 insertion reaction into the Au–Al bond in [$^tBu_3PAuAl(NON)$] complex,[25] with the Au–H bond (analogous to the Au–Al bond) acting as the actual nucleophile. Other components of the interaction are significantly smaller (see Figure S1 in the SI). Remarkably, the **1'**
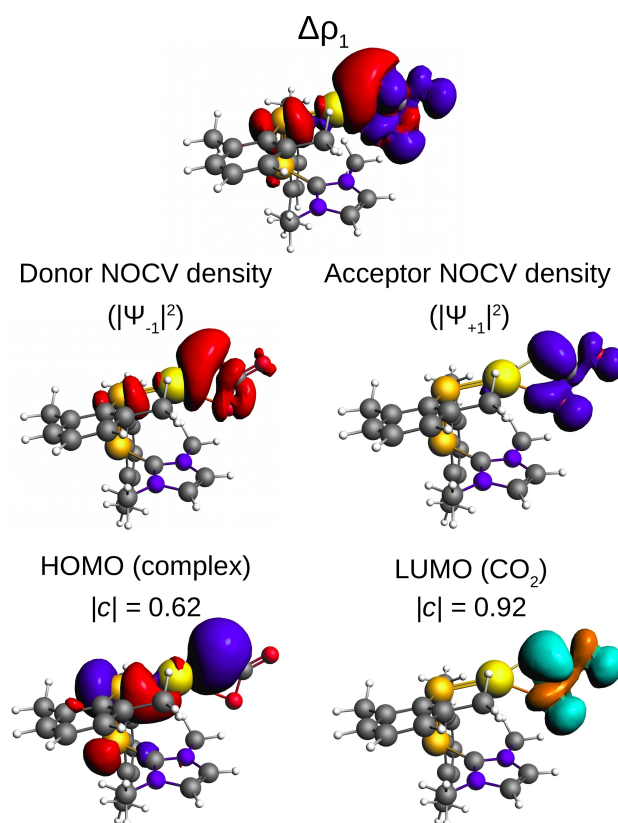

Figure 2. Breakdown of the donor ($|\Psi_{-1}|^2$) and acceptor ($|\Psi_{+1}|^2$) NOCV densities associated with the first NOCV deformation density, $\Delta\rho_1$, in the transition state TS involving the **1'** complex into the most important MOs of the **1'** and CO_2 fragments frozen at their TS geometry. The molecular orbitals mixing coefficients (c) are given. Isodensity values are 0.001 e au^{-3} for $\Delta\rho_1$, 0.002 e au^{-3} for NOCV densities and 0.03 e au^{-3} for MOs.

Chemistry–A European Journal

Research Article
doi.org/10.1002/chem.202303512

Chemistry Europe
European Chemical
Societies Publishing

HOMO involved in the interaction with CO_2 does contain contributions from the P–Au σ bond, thus suggesting a role of the ligand in the experimentally observed reactivity for this complex.

Moving to different ligands, we optimized the three key structures of the reaction (Scheme 3) for all the ligands depicted in Scheme 2: the hydride species, the transition state and the formate product. The result of this computational screening is that the concerted mechanism is valid in all the cases.

Interesting information can be derived by comparing the geometrical parameters of the different transition states. When L is particularly π acidic (**ox_NHC**, CO, and PF_3), the carbon dioxide bending is larger than 140°, with neutral ligands it is found to be around 137° and with anionic ones is between 133 and 136° (Table S6 in the SI). A remarkable exception is **1'**, which is globally neutral but the O–Ĉ–O angle in the corresponding TS shows a value of 133°, typical of anionic ligands. This can be explained on the basis of its "charge separation": the NHC moiety stabilizes a positive charge, while the phosphorus carries a formal negative charge (Scheme 1).

Information on the feasibility of the reaction can be derived by comparing the free energy difference between reactants and TSs ($\Delta G^{\ddagger}$) and between reactants and products (ΔG_{rxn}). The former spans a range between 3.9 and 39.8 kcal/mol, indicating a strong ligand effect, but it is interesting to note that ΔG_{rxn} is
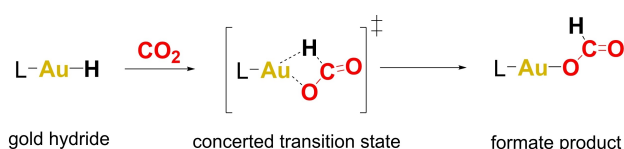
Scheme 3. Schematic representation of the reaction mechanism of monomeric gold hydrides with CO_2.

positive in many cases (Figure 3). The thermodynamic instability of the product is consistent with the fact that gold(I) hydrides are generally not able to activate CO_2. Negative values have been found for CN^-, PMe_2^- and [**NONAI**]⁻, of which only the latter can be really tested in laboratory. However, small, positive values of ΔG_{rxn} are even more interesting, as they could indicate a reversible (therefore, possibly catalytic) reaction as the **1'** complex. Other ligands with similar kinetic and thermodynamic values are [**O_NHC**]⁻ and NMe_2^-, of which only the former is a potential candidate for an experimental study. Other anionic ligands, especially [**R₃B_NHC**]⁻, seem to be promising candidates for an experimental study.

Notably, if the structure of **1'** is modified to avoid the zwitterionic character, both thermodynamic and kinetic parameters sensibly get worse (ΔG_{rxn} markedly positive, $\Delta G^{\ddagger}$ larger than 30 kcal/mol). This strongly confirms that the ability of
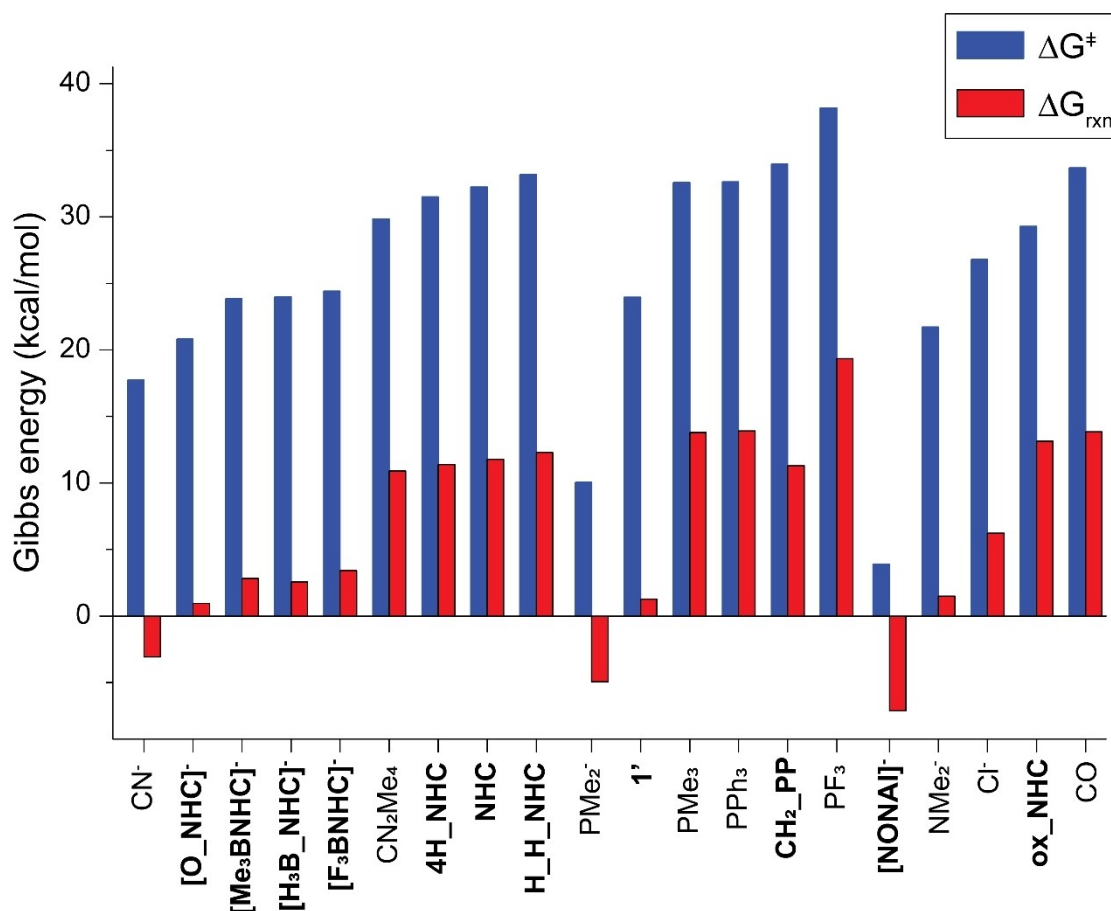

Figure 3. Activation ($\Delta G^{\ddagger}$) and thermodynamic (ΔG_{rxn}) parameters for the CO_2 activation by the [LAuH] species.

Chemistry–A European Journal

Research Article
doi.org/10.1002/chem.202303512

Chemistry Europe
European Chemical
Societies Publishing

carbene moiety to stabilize a positive charge is crucial for the CO_2 activation.

Therefore, we can conclude that anionic or zwitterionic ligands should be designed for this reaction. We just note here that $\Delta G^{\ddagger}$ and the activation electronic energy ($\Delta E^{\ddagger}$) correlate quite well each other ($r^2 = 0.9640$) and using one or the other has minimal effect on correlations.

To better understand the ligand effect in the reactivity of gold–hydride complexes, it is important to characterize the Dewar–Chatt–Duncanson (DCD) components[52] of both the Au—H and L—Au bonds. With respect to the gold–hydrogen bond, the [LAuH] complexes can be fragmented into two distinct ways: $[LAu]^{+/0}\cdots[H]^-$ (dative bond) and $[LAu]^{\bullet 0/-}\cdots[H]^{\bullet}$ (covalent bond), whereby the formal charge on the gold fragment depends on the nature of the ligand. The best possible fragmentation can be determined on the basis of the Energy Decomposition Analysis.[53,54] In particular, it has been demonstrated that the most realistic and suitable bond fragmentation is the one that has the least negative value of orbital interaction (ΔE_{oi}).[54] In the case of [**NHC**AuH], for instance, the values of ΔE_{oi} are −90.7 and −76.2 kcal/mol for the ionic and covalent fragmentations, respectively, allowing to consider the latter more suitable and to formally consider the Au—H bond in this complex as a covalent bond. Relying on this approach, we found out that the covalency of the Au—H bond is a common characteristic when the ligand is neutral and

becomes more borderline with anionic ligands (see Table S1–S3 for comprehensive energy data). Shifting to the ligand–gold bond, instead, we verified the best fragmentation scheme by testing some representative complexes among the whole group (see Table S4), finding that the best fragmentation is the $[L]^{0/-}\cdots[AuH]$ one.

The assessment of the suitable L—Au bond fragmentation allowed us to quantify the L—AuH DCD components of all the complexes formed with ligands listed in Scheme 2 through the CD–NOCV analysis. For each complex, a series of NOCV ($\Delta\rho_k$, k = 1…n) was derived, and from their integration along the L—Au axis, a value for the associated charge transfer (CT_k) was evaluated. The main results are displayed in Figure 4. Positive values refer to L→Au donation contributions, negative values to L←Au back–donation ones.

In almost all the cases the CT1 is relative to the L→AuH σ donation and it is much larger than the L←AuH π back–donation (generally CT2 and CT3). Some exceptions are strongly π acidic ligand **ox_NHC**, for which CT1 is a back–donation component. For **CO**, the total back–donation (CT2 + CT3) is larger than the donation component (CT1). The chloride and NMe_2^- ligands possess also π L→Au donation components, in agreement with their π basic nature.

Beyond the present selection of ligands and the consideration made before, it would be extremely useful to provide "quantitative" guidelines for the rational design of new
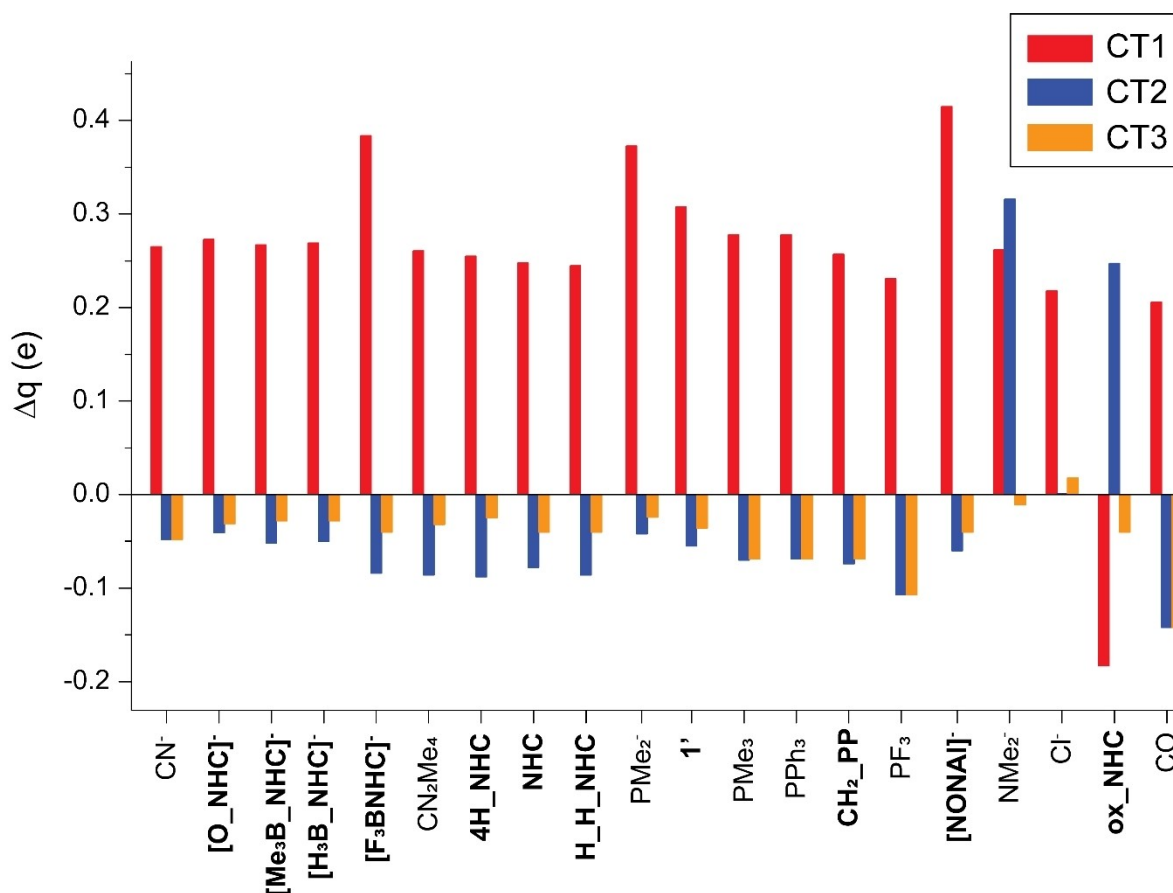

Figure 4. CD-NOCV components of the L—AuH bond. Positive values refer to L→AuH donations, negative ones to L←AuH back–donations.

Chemistry–A European Journal

Research Article
doi.org/10.1002/chem.202303512

Chemistry Europe
European Chemical
Societies Publishing

catalysts. To this aim, a deeper insight is necessary. Considering that a more basic hydride is expected to better activate CO_2 we analyzed the Voronoi Deformation Density (VDD) atomic charges[55] on Au and H in all the complexes (Table S7 in the SI). From a general and simple chemical intuition, it is reasonable to imagine that a higher gold–hydrogen polarization would lead to an easier reactivity towards CO_2. However, the correlations between $\Delta G^{\ddagger}$ and VDD charges (or Au–H polarization) are not satisfactory (Figures S2 in the SI), even if the qualitative trend is coherent with this hypothesis. This is not a surprising result, as atomic charges are very method–dependent.

A more reliable method to analyze the electronic ligand effect on the hydride is the use of the CD–NOCV approach. Analogously, the simple correlation between the L–AuH bond components (displayed in Figure 4) and $\Delta G^{\ddagger}$ (Figure 3) is unsatisfactory (see Figure S3 in the SI). This likely depends on the fact that DCD components are evaluated between the ligand and gold in the isolated complexes, which is far from the reactive site. The CD curves have the great advantage that they give information about any region of interest and the electronic effect of L on the AuH fragment can be evaluated directly on the hydride, obtaining one value for each NOCV bond component. For example, in the case of **NHC**–AuH, the values of Δq_{H1}, Δq_{H2}, and Δq_H (that corresponds to the sum of all the NOCV components) can be obtained by integrating the CD curves at the z coordinate of the hydride (Figure 5a).

In this framework, Δq_{H1-2} represent how much the electronic density around the hydride is modified upon the coordination of the ligand, decomposed with the same scheme used to determine the DCD bond components. Therefore, Δq_{H1} generally describes the response of the hydride to the L→Au σ donation, and Δq_{H2} describes the response of the hydride to the π back–donation. The correlation of Δq_{H1} with $\Delta G^{\ddagger}$ is indeed better than the previous ones ($r^2 = 0.8766$, see Figure 6a and S4 in the SI). This is in agreement with the chemical intuition: more donating ligands favor the reaction. The correlation is good enough to be used in a computational screening, with a largest error of 6.2 kcal/mol (L = **NONAI⁻**) and a mean absolute error of 2.7 kcal/mol. Being Δq_{H1} computed from the isolated hydride, the transition state optimization (which is more time consuming) would be not necessary.

However, the picture is not completely satisfactory, especially because Δq_{H2} is constantly null (Figure 5a) and does not provide any information. In order to make a step further and better characterize the ligand effect during the reaction, we used the TS geometry for the same analysis (Figure 5b), obtaining $\Delta q'_{H1}$ and $\Delta q'_{H2}$, and $\Delta q'_H$ for the sum of all the components. Furthermore, in this case $\Delta q'_{H2}$ is generally small but not negligible at the coordinate of the hydride, allowing us to have information also from the effect of the L←Au back–donation. Finally, we should note that $\Delta q'_H$ is not purely relative to the hydride species, but also to one oxygen of the CO_2, which has a very similar z coordinate (Figure 5b). The inclusion of carbon dioxide moiety in this analysis results to be fundamental for the
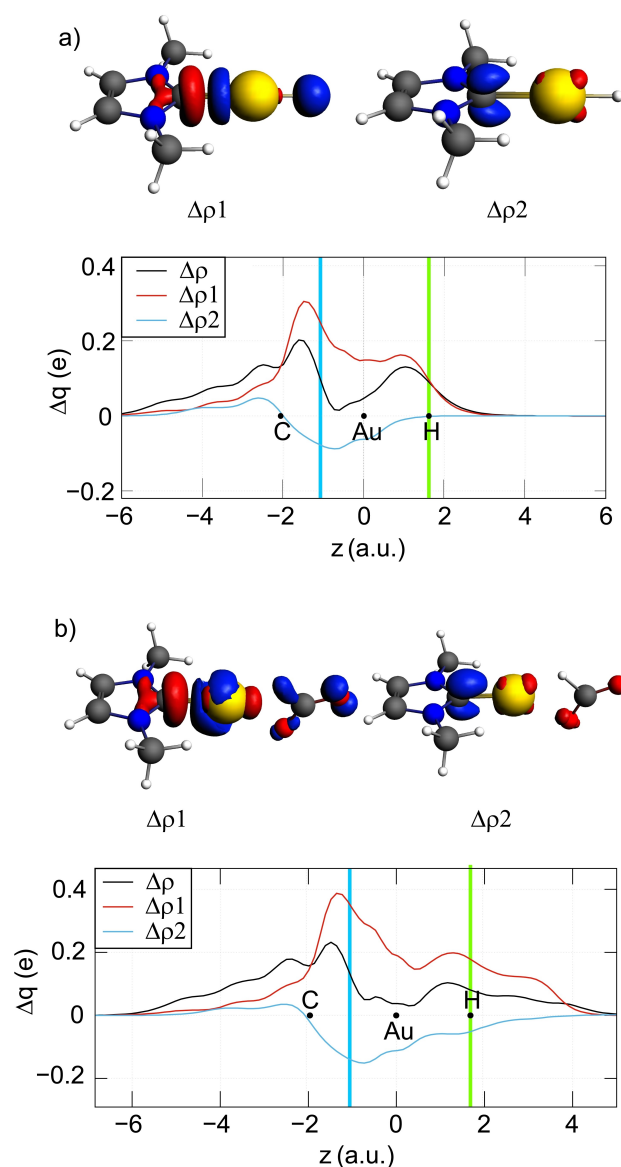

Figure 5. Above: isodensity surfaces (5 me a.u.$^{-3}$) for the deformation maps relative to $\Delta \rho_1$ and $\Delta \rho_2$ of a) **NHC**–AuH (interacting fragments: [**NHC**] and [AuH]) and b) **NHC**–AuH–CO_2 TS (interacting fragments: [**NHC**] and [AuHCO$_2$]). Blue (red) regions indicate electron charge accumulation (depletion). Below: Charge Displacement (CD–NOCV) curves associated with the $\Delta \rho_1$ and $\Delta \rho_2$ NOCV deformation densities and with the total $\Delta \rho$. Positive (negative) values of the curve indicate right-to-left (left-to-right) charge transfer, black dots represent the atom z coordinates. The light blue vertical line denotes the coordinates where CT$_1$, CT$_2$, and CT are evaluated, the green vertical line where Δq_{H1}, Δq_{H2}, and Δq_H are measured.

correlation between the response of the hydride to the L→Au σ donation, $\Delta q'_{H1}$, and $\Delta G^{\ddagger}$ which is very good if some outliers are excluded (Figure 6b). In particular, the outliers are NMe$_2$⁻, Cl⁻, **ox_NHC** and **CO**. The meaning of the correlation is the same as before: strong electron–donating ligands favor the reaction, as the hydride is more nucleophilic. The outliers are utterly important to understand why the model works in most cases while it fails in some other, isolated, cases.
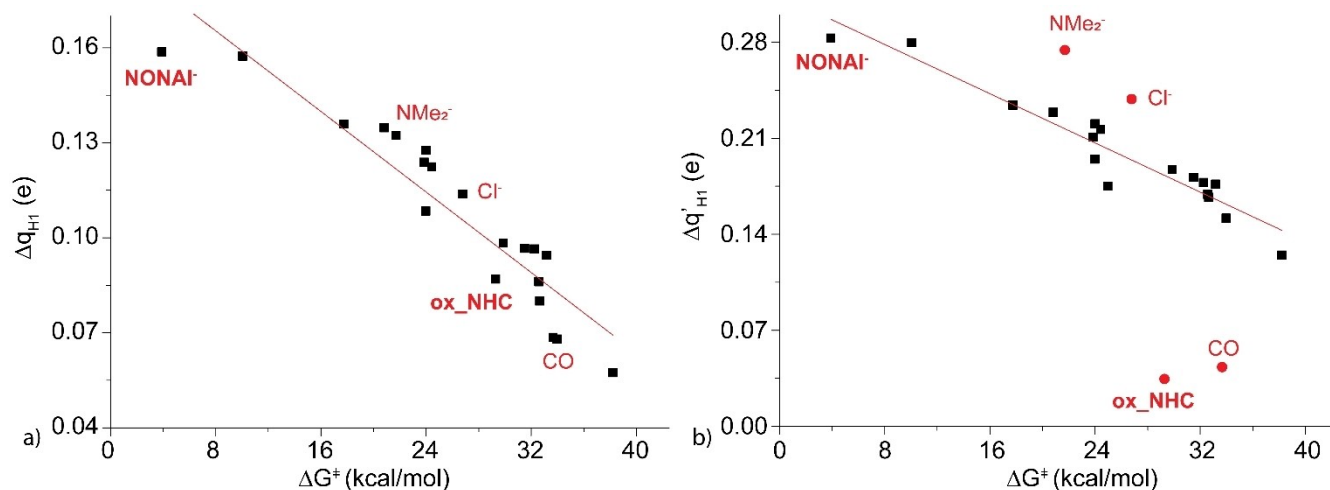
Chemistry–A European Journal

Research Article
doi.org/10.1002/chem.202303512

Chemistry Europe
European Chemical
Societies Publishing

Figure 6. a) Correlation between Δq_{H1} and $\Delta G^{\ddagger}$. The best fit equation is $\Delta q_{H1} = -0.00318 \cdot \Delta G^{\ddagger} + 0.1908$ ($r^2 = 0.8766$). b) Correlation between $\Delta q'_{H1}$ and $\Delta G^{\ddagger}$. The correlation factors r^2 are 0.9400 (only relative to the black squares) and 0.4952 (all data). Relevant ligands are indicated in red.

Firstly, we can see that some outliers show a positive deviation (their value of $\Delta q'_H$ is "too high" with respect to other ligands with similar $\Delta G^{\ddagger}$, such as NMe_2^- and Cl^-), while others show negative deviations (such as CO and **ox_ NHC**).

To get a deeper insight, we can compare the NOCV deformation maps of a ligand well described by our correlation with those of the outliers (Figure 7). Indeed, they are markedly different. When L=PMe$_3$, $\Delta\rho_1$ shows only accumulation regions around CO_2 (Figure 7a), while when L = **ox_NHC** (Figure 7b) (or CO, see Figure S5 in the SI) the ligand is so π acidic that a depletion region appears around CO_2 also in $\Delta\rho_1$, making $\Delta q'_H$ less negative and generating the deviation from the correlation.[56] In general, the NOCV methods seems unable to discriminate donation and back–donation in these particular cases. As a confirmation, the sum of $\Delta\rho_1$ and $\Delta\rho_2$ is qualitatively similar for L=PMe$_3$ or **ox_ NHC** (Figure S7).
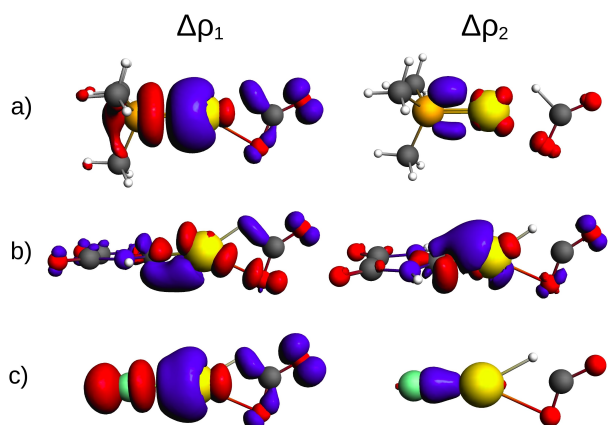
In the case of Cl^- and NMe_2^-, the main difference lies in $\Delta\rho_2$: in the deformation map when L=PMe$_3$, there is a depletion region at the oxygen atoms of CO_2 and at the gold (Figure 7a), consistent with the π L←Au back–donation component. On the contrary, Cl^- has no back–donation component and it acts as a donating ligand in all the components (Figure 7c). The NOCV deformation maps when L=NMe_2^- are very similar to those of chloride (see Figure S6 in the SI).

Remarkably, all these deviations from the trend are discernible by the visual analysis of NOCV deformation maps, and outliers can be easily recognized.

Conclusions

In this paper, we analyzed the ligand effect in the reaction between a molecular gold(I) hydride and CO_2, with the formation of the formate anion. This reaction is generally unfeasible and only one successful example is present in the literature, for which the yet unknown reaction mechanism was elucidated through this study. Our analysis points out that the obstacle for the reaction is generally thermody-namic in nature, and not kinetic, as the product is inherently unstable. However, in some cases, both thermodynamic and kinetics are favorable, especially in the case of anionic ligands, such as [**O_NHC**]$^-$, [**NONAI**]$^-$, and [**R$_3$B_NHC**]$^-$ which deserve in–depth experimental studies for stoichiometric and catalytic CO_2 activation. As in the case of ligand **1**, which experimentally demonstrated to work in this reaction,[17] also strongly polarized ligands with the negative pole close to gold, can be utterly useful.

The ligand effect on the activation barrier was also explored, finding out that most of the ligands can be grouped in the same correlation: in particular, the activation free energy linearly correlates with both Δq_{H1} and $\Delta q'_{H1}$, which describes how much the σ donation ability of the

Figure 7. Comparison between NOCV deformation maps (3 me a.u.$^{-3}$) for three different ligands: PMe$_3$ (a) which is well described by the correlation in Figure 5, **ox_NHC** (b) which shows a negative deviation, and the chloride (c) showing a positive deviation.

Chemistry–A European Journal

Research Article
doi.org/10.1002/chem.202303512

Chemistry Europe
European Chemical
Societies Publishing

ligand modifies the electron density at the hydride coordinate for the isolated hydride species and the TS, respectively. The computation of Δq_{H1} does not require the TS optimization, which can be time–consuming especially for large ligands, and the qualitative correlation already provides a good estimation of the activation barrier (mean absolute error = 2.7 kcal/mol). This is a useful tool for a computational screening aimed to rapidly locate most promising systems to be experimentally tested.

If the TS geometry is available, the correlation is better but, interestingly, a few ligands do not fit in this trend, such as the π-donor chloride and the π-acceptor [**ox_NHC**] ligands. Anyway, the outlier behavior can be rationalized analyzing the details of the NOCV output.

These results pave the way for focused experimental studies, having as target the synthesis of the few gold(I) hydrides that resulted promising here, and their reaction in the CO_2 activation. More in general, new ligands should be designed in order to have a strong L→Au σ donation, with preference for anionic or zwitterionic structures.

Acknowledgements

Conflict of Interests

The authors declare no conflict of interest.

Data Availability Statement

The data that support the findings of this study are available from the corresponding author upon reasonable request.

[1] Trends in Atmospheric Carbon Dioxide, Global Monitoring Laboratory, Webpage https://gml.noaa.gov/ccgg/trends/monthly.html (accessed 9 February 2024).

[2] Carbon Dioxide Insertion into Group 9 and 10 Metal-Element σ Bonds N. Hazari, J. E. Heimann, *Inorg. Chem.* **2017**, *56*, 13655–13678, doi:10.1021/acs.inorgchem.7b02315.

[3] M. Cokoja, C. Bruckmeier, B. Rieger, W. A. Herrmann, F. E. Kühn, *Angew. Chem. Int. Ed.* **2011**, *50*, 8510–8537, doi:10.1002/anie.201102010.

[4] T. J. Schmeier, G. E. Dobereiner, R. H. Crabtree, N. Hazari, *J. Am. Chem. Soc.* **2011**, *133*, 9274–9277, doi:10.1021/ja2035514.

[5] B. Mondal, F. Neese, S. Ye, *Inorg. Chem.* **2016**, *55*, 5438–5444, doi:10.1021/acs.inorgchem.6b00471.

[6] W. H. Bernskoetter, N. Hazari, *Eur. J. Inorg. Chem.* **2013**, *22(23)*, 4032–4041, doi:10.1002/ejic.201300170.

[7] H. Schwarz, *Coord. Chem. Rev.* **2017**, *334(112–123)*, doi:10.1016/j.ccr.2016.03.009.

[8] T. Fan, X. Chen, Z. Lin, *Chem. Commun.* **2012**, *48*, 10808–10828, doi:10.1039/c2cc34542k.

[9] H. W. Suh, T. J. Schmeier, N. Hazari, R. A. Kemp, M. K. Takase, *Organometallics* **2012**, *31*, 8225–8236, doi:10.1021/om3008597.

[10] C. Yin, Z. Xu, S. Y. Yang, S. M. Ng, K. Y. Wong, Z. Lin, C. P. Lau, *Organometallics* **2001**, *20*, 1216–1222, doi:10.1021/om000944x.

[11] N. M. Rezayee, C. A. Huff, M. S. Sanford, *J. Am. Chem. Soc.* **2015**, *137*, 1028–1031, doi:10.1021/ja511329m.

[12] C. A. Huff, M. S. Sanford, *J. Am. Chem. Soc.* **2011**, *133*, 18122–18125, doi:10.1021/ja208760j.

[13] The Gold-Hydrogen Bond, Au—H, and the Hydrogen Bond to Gold, Au⋯H—X. H. Schmidbaur, H. G. Raubenheimer, L. Dobrzańska, *Chem. Soc. Rev.* **2014**, *43*, 345–380, doi:10.1039/c3cs60251f.

[14] D. A. Roşca, J. Fernandez-Cestau, D. L. Hughes, M. Bochmann, *Organometallics* **2015**, *34*, 2098–2101, doi:10.1021/om501165z.

[15] C. A. Gaggioli, L. Belpassi, F. Tarantelli, D. Zuccaccia, J. N. Harvey, P. Belanzoni, *Chem. Sci.* **2016**, *7*, 7034–7039, doi:10.1039/C6SC02161A.

[16] C. A. Gaggioli, L. Belpassi, F. Tarantelli, J. N. Harvey, P. Belanzoni, *Dalt. Trans.* **2017**, *46*, 11679–11690, doi:10.1039/c7dt02170d.

[17] D. Dhara, S. Das, S. K. Pati, D. Scheschkewitz, V. Chandrasekhar, A. Jana, *Angew. Chem. Int. Ed.* **2019**, *58*, 15367–15371, doi:10.1002/anie.201909798.

[18] D. Dhara, D. Scheschkewitz, V. Chandrasekhar, C. B. Yildiz, A. Jana, *Chem. Commun.* **2021**, *57*, 809–812, doi:10.1039/d0cc05461e.

[19] L. Benhamou, V. César, H. Gornitzka, N. Lugan, G. Lavigne, *Chem. Commun.* **2009**, *31*, 4720–4722, doi:10.1039/b907908d.

[20] Y. Wang, Y. Xie, M. Y. Abraham, P. Wei, H. F. Schaefer, P. V. R. Schleyer, G. H. Robinson, *J. Am. Chem. Soc.* **2010**, *132*, 14370–14372, doi:10.1021/ja106631r.

[21] M. Braun, W. Frank, C. Ganter, *Organometallics* **2012**, *31*, 1927–1934, doi:10.1021/om201235c.

[22] J. Hicks, A. Mansikkamäki, P. Vasko, J. M. Goicoechea, S. Aldridge, *Nat. Chem.* **2019**, *11*, 237–241, doi:10.1038/s41557-018-0198-1.

[23] D. Sorbelli, E. Rossi, R. W. A. Havenith, J. E. M. N. Klein, L. Belpassi, P. Belanzoni, *Inorg. Chem.* **2022**, *61*, 7327–7337, doi:10.1021/acs.inorgchem.2c00174.

[24] D. Sorbelli, L. Belpassi, P. Belanzoni, *Chem. Sci.* **2022**, *13*, 4623–4634, doi:10.1039/d2sc00630h.

[25] D. Sorbelli, L. Belpassi, P. Belanzoni, *J. Am. Chem. Soc.* **2021**, *143*, 14433–14437, doi:10.1021/jacs.1c06728.

[26] G. Ciancaleoni, F. Nunzi, L. Belpassi, *Molecules* **2020**, *25(300)*, doi:10.3390/molecules25020300.

[27] The Chemical Bond between Au(I) and the Noble Gases. Comparative Study of NgAuF and NgAu + (Ng=Ar, Kr, Xe) by Density Functional and Coupled Cluster MethodsL. Belpassi, I. Infante, F. Tarantelli, L. Visscher, *J. Am. Chem. Soc.* **2008**, *130*, 1048–1060, doi:10.1021/ja0772647.

[28] G. Bistoni, L. Belpassi, F. Tarantelli, *J. Chem. Theory Comput.* **2016**, *12*, 1236–1244, doi:10.1021/acs.jctc.5b01166.

[29] R. F. Nalewajski, J. Ozek, *Int. J. Quantum Chem.* **1994**, *51*, 187–200, doi:10.1002/qua.560510403.

[30] A. Michalak, M. Mitoraj, T. Ziegler, *J. Phys. Chem. A* **2008**, *112*, 1933–1939, doi:10.1021/jp075460u.

[31] M. P. Mitoraj, A. Michalak, T. A. Ziegler, *J. Chem. Theory Comput.* **2009**, *5*, 962–975, doi:10.1021/ct800503d.

[32] D. Sorbelli, P. Belanzoni, L. Belpassi, J. W. Lee, G. Ciancaleoni, *J. Comput. Chem.* **2022**, *43*, 717–727, doi:10.1002/jcc.26829.

[33] G. Bistoni, S. Rampino, F. Tarantelli, L. Belpassi, *J. Chem. Phys.* **2015**, *142*, 084112, doi:10.1063/1.4908537.

[34] G. Ciancaleoni, L. Belpassi, *J. Comput. Chem.* **2020**, *41*, 1185–1193, doi:10.1002/jcc.26165.

[35] G. Marrazzini, C. Gabbiani, G. Ciancaleoni, *ACS Omega* **2019**, *4*, 1344–1353, doi:10.1021/acsomega.8b03330.

[36] E. Buttarazzi, F. Rosi, G. Ciancaleoni, *Phys. Chem. Chem. Phys.* **2019**, *21*, 20478–20485, doi:10.1039/c9cp03811f.

[37] F. Neese, F. Wennmohs, U. Becker, C. Riplinger, *J. Chem. Phys.* **2020**, *152*, 224108, doi:10.1063/5.0004608.

[38] F. Neese, Software Update: The ORCA Program System-Version 5.0. *Wiley Interdiscip. Rev. Comput. Mol. Sci.* **2022**, *12*, doi:10.1002/wcms.1606.

[39] E. Van Lenthe, E. J. Baerends, J. G. Snijders, *J. Chem. Phys.* **1994**, *101*, 9783–9792, doi:10.1063/1.467943.

[40] E. van Lenthe, E. J. Baerends, J. G. Snijders, *J. Chem. Phys.* **1993**, *99*, 4597–4610, doi:10.1063/1.466059.

[41] E. Van Lenthe, *J. Chem. Phys.* **1999**, *110*, 8943–8953, doi:10.1063/1.478813.

[42] D. A. Pantazis, X. Y. Chen, C. R. Landis, F. Neese, *J. Chem. Theory Comput.* **2008**, *4*, 908–919, doi:10.1021/ct800047t.

[43] A. D. Becke, *Phys. Rev. A* **1988**, *38*, 3098–3100, doi:10.1103/PhysRevA.38.3098.

Chemistry–A European Journal

Research Article
doi.org/10.1002/chem.202303512

Chemistry Europe
European Chemical
Societies Publishing

[44] J. P. Perdew, *Phys. Rev. B* **1986**, *33*, 8822–8824, doi:10.1103/PhysRevB.33.8822.

[45] S. Grimme, J. Antony, S. Ehrlich, H. A. Krieg, *J. Chem. Phys.* **2010**, *132*, 5585, doi:10.1063/1.3382344.

[46] S. Grimme, S. Ehrlich, L. Goerigk, *J. Comput. Chem.* **2011**, *32*, 1456–1465, doi:10.1002/jcc.21759.

[47] C. C. Pye, T. Ziegler, *Theor. Chem. Acc.* **1999**, *101*, 396–408, doi:10.1007/s002140050457.

[48] L. Zhao, M. von Hopffgarten, D. M. Andrada, G. Frenking, *Wiley Interdisciplinary Reviews: Computational Molecular Science* John Wiley & Sons, Ltd May 1, **2018**, p e1345, doi:10.1002/wcms.1345.

[49] G. Te Velde, F. M. Bickelhaupt, E. J. Baerends, C. Fonseca Guerra, S. J. A. van Gisbergen, J. G. Snijders, T. Ziegler, *J. Comput. Chem.* **2001**, *22*, 931–967, doi:10.1002/jcc.1056.

[50] M. De Santis, S. Rampino, H. M. Quiney, L. Belpassi, L. Storchi, *J. Chem. Theory Comput.* **2018**, *14*, 1286–1296, doi:10.1021/acs.jctc.7b01077.

[51] PYCUBESCD, Github.Com/BERTHA-4c-DKS/Pycubescd.

[52] J. Chatt, L. A. Duncanson, *J. Chem. Soc.* **1953**, 2939–2947, doi:10.1039/jr9530002939.

[53] M. von Hopffgarten, G. Frenking, *Wiley Interdiscip. Rev.: Comput. Mol. Sci.* **2012**, *2*, 43–62, doi:10.1002/wcms.71.

[54] P. Jerabek, P. Schwerdtfeger, G. Frenking, *J. Comput. Chem.* **2019**, *40*, 247–264, doi:10.1002/jcc.25584.

[55] C. Fonseca Guerra, J. W. Handgraaf, E. J. Baerends, F. M. Bickelhaupt, *J. Comput. Chem.* **2004**, *25*, 189–210, doi:10.1002/jcc.10351.

[56] C. A. Gaggioli, G. Bistoni, G. Ciancaleoni, F. Tarantelli, L. Belpassi, P. Belanzoni, *Chem. A Eur. J.* **2017**, *23*, 7558–7569, doi:10.1002/chem.201700638.